Synthesis and characterization of microcrystalline cellulose-graft-poly(methyl methacrylate) copolymers and their application as rubber reinforcements

Fei Deng,[1] Xin Ge,[1] Yinhang Zhang,[1] Mei-Chun Li,[2] Ur Ryong Cho[1]

[1]School of Energy, Materials and Applied Chemical Engineering, Korea University of Technology and Education, Cheonan 330708, Republic of Korea

[2]School of Renewable Natural Resources, Louisiana State University AgCenter, Baton Rouge, Louisiana 70803

Correspondence to: U. R. Cho (E-mail: urcho@koreatech.ac.kr)

ABSTRACT: In this study, redox-initiated free radical graft copolymerization of microcrystalline cellulose (MCC) and methyl methacrylate (MMA) has been carried out in aqueous media to develop a novel cellulose-based copolymer. Cerium ammonium nitrate was used as the initiator in the presence of nitric acid. Effects of monomer concentration, initiator concentration, polymerization time, and polymerization temperature on the graft parameters of copolymers were studied. The successful grafting copolymerization between MCC and MMA was validated through attenuated total reflection, wide-angle X-ray diffraction, field-emission scanning electron microscopy, and thermal gravimetric analysis. In comparison to native MCC, the resultant copolymers exhibited enhanced thermal stability and better compatibility with natural rubber, suggesting its potential application as reinforcement material in rubber industry. © 2015 Wiley Periodicals, Inc. J. Appl. Polym. Sci. **2015**, *132*, 42666.

INTRODUCTION

Cellulose, as the most abundant biopolymer, has attracted lots of attention due to its biodegradability and renewability. Cellulose and its derivatives can be used to produce various useful products, such as paper, reinforcing agent, flocculation agent, and rheological modifier.[1,2] Microcrystalline cellulose (MCC) originated from wood and cotton is widely applied in cosmetic, food, and other industries.[3] MCC is microsize hydrolyzed cellulose consisting of ordered regions (crystalline regions) and less-ordered regions (amorphous regions). The latter chemically hinges the cellulose nanocrystals together.[4] With the acid hydrolysis, the less-ordered regions are preferentially hydrolyzed, while the cellulose nanocrystals are released.[5] These cellulose nanocrystals with diameter ranging from 5 to 30 nm randomly aggregate together by the hydrogen bond. As a result, pores formed between these cellulose nanocrystals, and it has been reported that the pore size ranges from several nanometers to over 10 nm.[6] The size variation is expected to affect the functional properties of microcrystalline cellulose. For example, thanks to the porous structure, the specific surface area of MCC is about 2.50 m²/g,[7] which could be a favorable factor for surface modification. However, MCC cannot be uniformly dispersed in most nonpolar media due to its hydrophilic nature.[8,9]

To overcome the shortcoming, several surface modification methods, such as oxidation, silylation, esterification, etherification, and polymer grafting, have been applied. Among these methods, polymer grafting is one of the most effective techniques for transforming its superficial properties without changing its inherent properties.[10,11]

Till now, many techniques for graft copolymerization of various monomers on cellulose have been developed, including ring-opening polymerization,[12] free radical polymerization,[13] reversible addition-fragmentation polymerization,[14] nitroxide-mediated polymerization, and atom transfer radical polymerization.[15] Among them, free radical copolymerization initiated by ammonium cerium(IV) nitrite ($(NH_4)_2Ce(NO_3)_6$, CAN) in aqueous media has been thoroughly investigated for the grafting of polysaccharides,[16] such as cellulose and starch. For the graft copolymers, the graft ratio is a significant parameter, which strongly affects the surface characteristics of modified cellulose. Therefore, it is very essential to study how the grating ratio can be tailored by controlling the reaction parameters, such as monomer/cellulose ratio, concentration of initiator, time, and temperature. There are mainly two methods for the determination of graft ratio, including acid hydrolysis method and TGA method. With the first method, many factors influenced the acid hydrolysis

process, such as acid type,[17,18] acid concentration,[19] hydrolysis temperature,[17,20] and hydrolysis time,[17,20] leading to inaccurate results. Due to the simple and fast processing, the TGA method seems to be more suitable for determining the graft ratio of copolymers than the acid hydrolysis method. Indeed, the TGA method has been widely used to determine the graft ratio of modified cellulose microfibrils,[21] starch,[22] carbon nanotube,[23] and porous silica particles[24] in recent years.

Polymer composites are usually composed of two materials with different properties. The incorporation of reinforcing fillers into the polymer matrix can significantly improve the thermal, mechanical, wear, friction, and barrier properties. Up to now, various fillers, such as carbon black,[25] carbon nanotubes,[26] graphene oxide,[27] biomass carbon,[28] silica,[29] and nanoclay[30] have been used to prepare polymer composites with high performances. Considering the renewability and biodegradability, the application of sustainable cellulose in polymer composites is preferred. In recent years, cellulose has been compounded into different polymer matrixes, such as poly(methyl methacrylate),[31] poly(vinylidene fluoride),[32] and natural rubber.[33,34] Among them, natural rubber (NR) is one of the most widely used biopolymers.

The use of native cellulose to reinforce rubber composites has been widely reported. Previous studies showed that the reinforcing ability of native cellulose was very limited due to the poor interfacial interaction with rubber matrix.[35-37] To overcome this drawback, several efforts have been made to chemically modify cellulose.[38-40] The modified cellulose had better reinforcement in rubber matrix than native cellulose. For example, higher tear strength, tensile strength, and tensile modulus were achieved in modified cellulose reinforced natural rubber composites.[38-40] Methyl methacrylate (MMA) is a cheap, nontoxic, and active monomer, which has been widely used for surface modification of various fillers, such as starch,[19] cellulose,[17,18] carbon nanotube,[41] and clay.[42] For instance, a plenty of literatures reported the preparation of cellulose-*graft*-poly (methyl methacrylate) (MCC-*g*-PMMA) and discussed the effect of reaction parameters on the graft parameters of cellulose;[17-22] however, to the best of our knowledge, the use of MCC-*g*-PMMA as reinforcing filler in natural rubber matrix has been barely reported. Furthermore, since the grafts on the modified filler played a crucial role in enhancing interfacial interaction between modified filler and polymer matrix, the investigation on how the final performance of MCC-*g*-PMMA/NR composites influenced by the amounts of PMMA grafts is of great scientific interest and significance. However, few literatures systematically reported how the parameters of modification reaction influenced on the graft parameters of MCC-*g*-PMMA and eventually affected the final performance of MCC-*g*-PMMA/NR composites. In this work, the MCC-*g*-PMMA copolymers were achieved by CAN-initiated free radical polymerization of MCC and MMA in aqueous media. The effects of monomer ratio, reaction time, reaction temperature, and initiator concentration on the graft parameters of MCC-g-PMMA copolymers were studied. Two methods, i.e., acid hydrolysis and TGA methods were employed to determine the graft parameters and their results were compared. Attenuated total reflection (ATR), wide-angle X-ray diffraction (WXRD), field-emission scanning electron microscopy (FE-SEM), and thermal gravimetric analysis (TGA) were used to analyze the influence of graft parameters on the chemical structure, crystallinity, surface morphology, and thermal stability of MCC-g-PMMA, respectively. The application of MCC-g-PMMA with different amounts of PMMA grafts in NR was further studied, and their vulcanization and mechanical properties were evaluated.

EXPERIMENTAL

Materials

MCC with length 20–100 μm was purchased from Daejung Chemicals & Metals Cooperation (South Korea). MMA was provided by Duksan Pure Chemical cooperation (South Korea). Ammonium cerium (IV) nitrate was applied by Daejung Chemicals & Metals Cooperation (South Korea). Acetone was purchased from Samchun Pure Chemical Cooperation (South Korea). Tetrahydrofuran (THF) was purchased from Avantor Performance Material (USA). Hydrochloric acid (35%), nitric acid (60%), and perchloric acid (60–62%) were purchased from Duksan Pure Chemicals (South Korea). Natural rubber (NR) latex was provided by Korea Kumho Petrochemical Company (KKPC, South Korea). Stearic acid (above 95.0%), zinc oxide (above 99.0%), and sulfur power (above 99.0%) were supplied by Daejung Chem (South Korea). *N*-Cyclohexyl-2-benzothiazolysulfenamide (CBS) and dibenzothiazole disulfide (DD) were purchased from T.C.I. (Japan). All the chemicals and rubber additives were used as received without further purification.

Graft Copolymerization

The graft copolymerization procedure was based on the method described by Littunen *et al.*[17] and Li *et al.*[43] In a typical experiment, a certain amount of MCC was added into 300 mL distilled water in a four-necked round-bottom flask and mechanically stirred for 10 min. Subsequently a known amount of CAN/nitric acid solution (nitric acid concentration 0.1 mol/L) and MMA monomers were added into the suspension with stirring for 30 min. The copolymerization was carried out for 3 h at 45°C in a water bath under nitrogen atmosphere. After the reaction, the suspension was filtered and dried in the oven at 70°C for 12 h. The dried product was extracted using acetone in a Soxhlet apparatus for 72 h to remove the homopolymers. Finally the extracted product was dried and weighed.

Isolation of Grafted PMMA

In order to obtain the grafted PMMA, the extracted microcrystalline cellulose-graft-poly(methyl methacrylate) (MCC-*g*-PMMA) copolymers were hydrolyzed in 10 wt % HCl solution at boiling point for 5 h. Then 10 mL perchloric acid was added into the solution with stirring for 30 min,[43] followed by filtering the hydrolyzed products and drying at 70°C until the weight kept constant.

The results were used to calculate the graft ratio (G_R), graft efficiency (G_E), polymer weight fraction (W_G), and monomer conversion (C) with eqs. (1)–(4).

$$Graft\ ratio\ (G_R) = \frac{m_G}{m_C} \times 100\% \qquad (1)$$

$$Graft\ efficiency\ (G_E) = \frac{m_G}{m_P + m_G} \times 100\% \qquad (2)$$

$$Polymer\ weight\ fraction\ (W_G) = \frac{m_G}{m_C + m_G} \times 100\% \qquad (3)$$

$$Conversion\ (C) = \frac{m_G + m_P}{m_F} \times 100\% \qquad (4)$$

where m_G is the mass of the grafted polymer; m_C is the mass of cellulose; m_P is the mass of the homopolymer; and m_F is the mass of the fed monomer.

Characterization of Graft Copolymers

Determination of Molecular Weights. The number average molecular weight ($\overline{Mn}$), weight average molecular weight ($\overline{Mw}$), and polydispersity index ($\overline{D}$) of the grafted PMMA were determined by gel permeation chromatography (GPC, 1200 series, Agilent Technologies), which equipped with Refractive Index Detector, isocratic pump, PLgel GPC columns (5 μm MIXED-C, 300 × 7.5 mm) and thermostatted column compartment according to ASTM method E-1303-95. The measurement was conducted with response time of 4s and flow rate of 1.0 mL/min at an optics temperature of 35°C. THF was used as an eluent, and the calibration curve was obtained with polystyrene standards.

Attenuated Total Reflection (ATR) Analysis. The MCC and MCC-*g*-PMMA were recorded on an ATR spectrum (Perkin Elmer spectrum 1000) to verify the function groups. The frequency ranges from 400 to 4000 cm^{-1} with a resolution of 4.0 cm^{-1}.

Field Emission Scanning Electron Microscopy (FE-SEM) Observation. The surface morphology of the MCC and MCC-*g*-PMMA was investigated using FE-SEM (JSM-7500, JEOL). All the samples were sputter-coated with gold before the test.

Thermal Gravimetric Analysis(TGA). The grafting amount and thermal stability of the graft copolymer were investigated using TGA (PerkinElmer TGA 4000), in nitrogen atmosphere at a flow rate of 20 mL/min. The temperature ranges from ambient temperature to 600°C at a heating rate of 20°C/min.

Wide-Angle X-ray Diffraction (WXRD). WXRD patterns of MCC-*g*-PMMA were measured using WXRD (Empyrean, PANalytical) at 25°C. The WXRD data were generated by a diffractometer with Cu Kα radiation ($\lambda = 1.542$ Å) at 40 kV and 30 mA over the angular range $2\theta = 5°$–$50°$, with a step size of 2°min^{-1}. The degree of crystalline index (CI, %) for each sample was evaluated using eq. (5):

$$CI = (A_c/A_a) \times 100\% \qquad (5)$$

where A_c is the area of the crystalline reflection and A_a is the area subtending the whole diffraction profile.

Application of MCC-*g*-PMMA as NR Reinforcements

Compounding. The microcrystalline cellulose-*graft*-poly(methyl methacrylate)/natural rubber (MCC-*g*-PMMA/NR) compounds were prepared by directly mixing the MCC-*g*-PMMA with NR latex. The mixtures were vigorously stirred for 30 min at 1000 rpm to make a well dispersion of MCC-*g*-PMMA, and then dried in an oven at 70°C until the weight kept constant. Compounding was conducted on a two-roll mixing mill. The
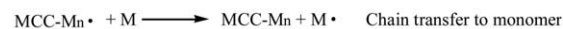
Scheme 1. Mechanism of cerium initiated graft copolymerization and homopolymerization.

dried compounds were formulated with the conventional elastomeric additives, such as sulfur, zinc oxide, stearic acid, accelerator n-cyclohexyl-2-benzothiazole sulfenamide (CBS), and accelerator dibenzothiazole disulfide (DD). The compounding formulation is as follows: NR, 100 phr; MCC-*g*-PMMA, 5 phr; sulfur, 2 phr; zinc oxide, 3 phr; straric acid, 1 phr; CBS, 2 phr; DD, 0.5 phr. Note that sulfur and accelerators were mixed in the final step to avoid prevulcanization. The vulcanization characteristics of compounds were determined using a MDR 2020 Reometer (Myung Ji Tech, South Korea) at 140°C. Finally, the compounds were vulcanized under 10 MPa for the optimum cure time at 140°C in a heating press machine. The thickness of the specimens was about 1 mm. For the purpose of comparison, neat NR and MCC/NR were also prepared.

Characterization of MCC-g-PMMA/NR. Vulcanization characteristics of compounds, including minimum torque (M_L), maximum torque (M_H), scorch time (t_{S2}), and optimum cure time (t_{90}) were determined. Curing rate index (CRI) was employed to evaluate the cure rate of rubber compounds, which was calculated by the following equation:

$$CRI = \frac{100}{t_{90} - t_{S2}} \qquad (6)$$

Tensile tests were performed on a Tinius Oisen H5KT-0401 testing machine at a speed of 500 mm/min according to ASTM D412. Tear strength was also measured on the same machine at a speed of 50 mm/min according to ASTM D642. Shore A hardness of the specimens was obtained with Shore Durometer Type A according to ASTM D2240. Five different specimens were measured to get the average value.

RESULTS AND DISCUSSION

The mechanism for methyl methacrylate monomers graft copolymerization onto cellulose using CAN as initiator and the formation of homopolymers has been reported as shown in Scheme 1. During the graft copolymerization, the initiation occurs via a redox reaction as the cerium ion chelates with two adjacent hydroxyl groups in a cellulose chain, resulting in radical formation on an opened glucose ring.[17] And the formation of homopolymers in the reaction mixture was due to the chain transfer reactions operating between growing chains and monomer molecules.[44] Different reaction parameters on the graft were studied. The products were characterized by FTIR, WXRD,

Table I. Effect of the Cellulose-to-Methyl Methacrylate Monomer Ratio on Graft Copolymerization

Cellulose: monomer	G_R (%)	G_E (%)	W_G (%)	C (%)	G_R^a (%)	G_E^a (%)	W_G^a (%)	G_R^b (%)	$\overline{Mn}$ (e^5·g/mol)	$\overline{Mw}$ (e^5·g/mol)	$\overline{D}$
3 : 1	24.5	81.3	19.7	84.5	111.7	93.1	52.8	33.3	1.1593	3.8028	3.2803
2 : 1	26.6	78.5	21.0	71.6	156.4	92.2	61.2	50.0	2.0176	8.4161	4.1714
1 : 1	42.4	69.4	29.8	67.9	231.9	87.2	72.5	100.0	2.7351	8.6538	3.1640
1 : 2	60.3	58.7	37.6	63.1	360.0	76.8	78.3	200.0	2.8733	8.8991	3.0972
1 : 3	68.2	57.7	40.6	59.8	368.4	73.4	78.7	300.0	3.6388	10.129	2.7837

[a] Determined by acid hydrolysis method.
[b] Theoretical value.
CAN, 0.5 wt %, 45°C, 3 h.

SEM, and TGA. Furthermore, the application of copolymers as NR reinforcements has also been studied.

Effect of Reaction Parameters on the Graft Copolymerization
The effects of MCC/MMA ratio, reaction time, reaction temperature, and initiator concentration on graft parameters and molecular weight of grafted PMMA were investigated. Graft parameters, such as graft ratio (G_R), graft efficiency (G_E), polymer weight fraction (W_G), monomer conversion (C), and molecular weight, such as number average molecular weight ($\overline{Mn}$), weight average molecular weight ($\overline{Mw}$), and polydispersity index ($\overline{D}$) were summarized in Tables I and II.

Effect of the MCC/MMA Ratio on the Graft Copolymerization. In order to investigate the effect of MCC/MMA ratio on the graft parameters and molecular weight of grafted PMMA, the concentration of initiator CAN, reaction temperature, and time were fixed as 0.5 wt %, 45°C, and 3 h, respectively. The comparison between hydrolysis and TGA method to get the graft parameters was investigated, as shown in Table I. The graft ratio determined by acid hydrolysis method was much higher than that determined by the TGA method, which was even higher than the theoretical value. Moreover, the G_E and W_G obtained by hydrolysis method were also higher than those determined by the TGA method. The reason was that the grafted polymer chains formed a coating, which significantly hindered the hydrolysis of cellulose. Therefore, it was concluded that the TGA method might give a more accurate result than the hydrolysis method for determining the graft parameters.

The effect of MCC/MMA ratio on the grafting parameters is given in Table I. With the increase in the MMA monomer concentration, both G_R and W_G were increased. This is because that an increase in monomer concentration led to the accumulation of monomer molecules in close proximity to the substrate backbone.[45] However, at a higher concentration, a large fraction of monomers was used for the formation of homopolymers due to the increased chain transfer reaction, resulting in the reduction of G_E. In addition, the monomer conversion also decreased, due to constant concentration of CAN.

Table I also presents the effect of MCC/MMA ratio on the molecular weight of grafted PMMA. Both $\overline{Mn}$ and $\overline{Mw}$ of the grafted PMMA were increased with the increase in the MMA monomer concentration, which is in accordance with the G_R

results. On the contrary, the $\overline{D}$ value decreased slightly. Littunen et al.[17] also prepared nanofibrillated cellulose-graft-PMMA copolymers using CAN as initiator. They found that the grafted PMMA had $\overline{Mw}$ of approximately 200,000 g/mol. In this study, when the MCC/MMA ratio was $1/2$, the $\overline{Mw}$ was 889,910 g/mol. This is attributed to the fact that the specific surface area of MCC was much lower than nanofibrillated cellulose, causing a limited amount of grafting points on the surface of MCC. As a result, MMA monomers were continuously propagated on the limited grafting points, leading to very high $\overline{Mw}$ values.

Effect of Reaction Time on Graft Copolymerization. In order to investigate the effect of reaction time on the graft parameters and molecular weight of grafted PMMA, the MCC/MMA ratio, concentration of initiator CAN, and reaction temperature were fixed as 1/1, 0.5 wt %, and 45°C, respectively. Table II shows the effect of reaction time on the graft parameters and molecular weight of grafted PMMA. When the reaction time was before 0.5 h, the graft parameters increased sharply. Beyond 0.5 h, the increasing tendency was largely reduced. This was due to the depletion of the monomers in reaction mixture and the steric hindrance offered by the graft chains of sufficient length, which retards the interactions of the monomers with growing chains, as proposed by Gupta et al.[46] Hence, the rate of transfer of monomer to the growing chains was decreased, but was allowed to diffuse monomers and ceric ions at a slower rate. This observation suggested that the process of formation of new reactive sites on cellulose continued after 0.5 h, but at a slow rate. Furthermore, the graft parameters and molecular weight were all increased with the increase in the reaction time. The increasing trend resulted to longer and more grafted chains, and lesser homopolymers. The chain transfer reaction was reduced by the steric hindrance.[46] Therefore, the reaction time had a strong impact on the copolymerization.

Effect of Reaction Temperature on Graft Copolymerization. In order to investigate the effect of reaction temperature on the graft parameters and molecular weight of grafted PMMA, the MCC/MMA ratio, concentration of initiator CAN, and reaction time were fixed as 1/1, 0.5 wt %, and 3 h, respectively. As shown in Table II, very different with the effect of reaction time, the graft parameters and molecular weight were all decreased with increase in the temperature. Thus the grafted chains became shorter and lesser, and more homopolymers were formed. This is due to that as the temperature increased,

Table II. Effect of Reaction Time, Temperature, and Initiator Concentration on MCC-g-PMMA Graft Copolymerization

	Reaction time (h)				Reaction temperature (°C)				Initiator concentration (%)			
	0.5	1	3	5	35	45	55	65	0.2	0.5	0.8	2.0
G_R (%)	38.5	40.5	42.4	43.6	52.0	42.4	42.1	35.1	36.1	42.4	40.5	37.5
G_E (%)	65.3	67.3	69.4	71.2	75.5	69.4	65.0	60.4	65.8	69.4	65.7	63.5
W_G (%)	27.8	28.8	29.8	30.4	34.2	29.8	29.6	26.0	26.5	29.8	28.8	27.3
C (%)	65.4	66.2	67.9	70.0	67.6	67.9	68.2	67.7	60.6	67.9	68.3	69.6
$\overline{Mn}$ (e^5·g/mol)	1.2367	1.8275	2.7351	3.0113	2.8871	2.7351	2.4378	1.7226	1.9020	2.7351	2.6461	1.2633
$\overline{Mw}$ (e^5·g/mol)	6.0386	6.0686	8.6538	8.1540	9.5474	8.6538	8.8431	6.7380	5.7069	8.6538	8.5014	4.4199
$\overline{D}$	4.8826	3.3207	3.1640	2.7078	3.3069	3.1640	3.6274	3.9115	3.0005	3.1640	3.2128	3.4986

Cellulose-to-monomer ratio: 1 : 1, CAN 0.5 wt %, 45°C, 3 h.

the initiator became instable, resulting in less reactive sites, as suggested by Li et al.[43] Another reason was that with increase in the temperature, the rate of chain transfer and chain termination between graft chains and monomer molecules substantially increased, as indicated by Gupta et al.[46] Therefore, 35°C was considered as the optimal temperature for the grafting copolymerization.

Effect of Initiator Concentration on Graft Copolymerization. In order to investigate the effect of initiator concentration on the graft parameters and molecular weight of grafted PMMA, the MCC/MMA ratio, reaction temperature, and reaction time were fixed as 1/1, 45°C, and 3 h, respectively. As shown in Table II, except for the C, the graft parameters were all first increased and then decreased, as the initiator concentration increased. The molecular weight showed the same trend with the graft parameters. The increase in the graft parameters was attributed to the mass formation of active ceric(IV) ions in the presence of excess nitric acid, which initiated the graft reaction. In addition, more initial free radicals formed on the surface of cellulose, resulting to more graft chains and less homopolymers. At higher concentrations (>0.5 wt %), the graft parameters were decreased due to the decrease in ratio of nitric acid to CAN. As a result, a hydrated form of ceric(IV) ions were produced, which were not able to produce active sites onto the cellulose backbone.[47] Another possible reason was due to the fact that the ceric(IV) ions started participating in oxidative termination of the growing graft chains, when the concentration of the ceric ammonium nitrate beyond 0.5 wt %,[46] which could result to more chain transfer reaction. Therefore, 0.5 wt % was selected as the optimal initiator concentration for graft copolymerization.

Based on the above investigations, it can be therefore concluded that the optimal reaction parameter was determined as MCC/MMA = 1/1; initiator concentration = 0.5 wt %; reaction temperature = 35°C; and reaction time = 3 h. In the following section, the graft copolymerization was evidenced by ATR, XRD, FE-SEM, and TGA analyses.

Evidence of Graft Copolymerization

ATR Analysis. The chemical structures of the graft copolymers were characterized using ATR spectrum. The ATR spectra for MCC and MCC-g-PMMA with MCC/PMMA ratio of 3/1, 1/1, 1/3 after extraction were presented in Figure 1. MCC displays the O—H stretching band in the region of 3650–3000 cm^{-1}, the C—H stretching at 2900 cm^{-1}, and the C—O stretching at 1025 cm^{-1}. The ATR spectra of MCC-g-PMMA 1/3, 1/1, and 3/1 exhibited all the characteristic peaks of MCC. Additionally, the peak at 1723 cm^{-1} is attributed to the C=O stretching, which is characteristics of the —COO group from PMMA. The presence of new stretching band at 1723 cm^{-1} provided sufficient evidence for the successful graft copolymerization. In addition, MCC shows a stronger stretching band at 3346 cm^{-1}, corresponding to the abundant hydrogen bonded hydroxyl groups on the backbone. For MCC-g-PMMA, this peak intensity decreased with the increase in the graft ratio, owing to the decrease of O—H groups, which were gradually substituted by grafted PMMA. The peak intensity of C—O stretching at
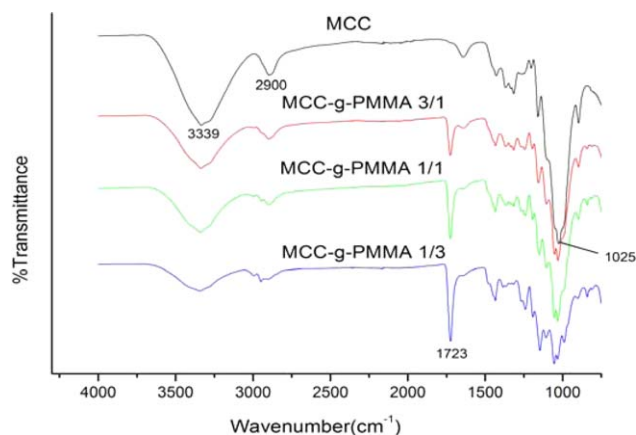
Figure 1. ATR-FTIR spectra of MCC, MCC-g-PMMA 3/1, MCC-g-PMMA 1/1, and MCC-g-PMMA 1/3 after extraction. [Color figure can be viewed in the online issue, which is available at wileyonlinelibrary.com.]

1025 cm^{-1} also decreased with increase in the graft ratio. On the contrary, the peak intensity of C=O stretching at 1723 cm^{-1} for MCC-g-PMMA 1/3, 1/1, and 3/1 were 86.78%, 80.89%, and 75.07% respectively, which decreased accordingly with decrease in graft ratio due to the increase in the quantity of ester groups.

WXRD Analysis. The WXRD profiles of MCC and MCC-g-PMMA were presented in Figure 2. The MCC exhibited three major diffraction peaks at 15.8°, 22.5°, and 34.5°. And the peak at 15.8° was two overlapped weaker diffraction peaks at 15.1° and 16.6°.[48] Thus the three diffraction peaks corresponded to the cellulose I crystallographic planes 110, 1$\bar{1}$0, 200, and 400, respectively.[49] In addition, the d-spacings of the three peaks were 0.56, 0.40, and 0.26 nm, respectively, indicating that the cellulose sample used in this study was cellulose I$_\beta$ type, which was monoclinic structure.[50] The grafted cellulose with different monomer ratio all presented the peak of 15.8°, 22.5°, and 34.5°, and the *CI* values of MCC, MCC-g-PMMA 3/1, MCC-g-PMMA 1/1, and MCC-g-PMMA 1/3 were 41.87%, 38.68%, 37.93%, and 31.72%, respectively. So the amorphous regions of copolymers increased with higher graft ratio.

Surface Morphology. The surface appearances of MCC and MCC-g-PMMA 1/1 after extraction were observed by FE-SEM as shown in Figure 3. The length of MCC was about 20–100 μm. The pore structure of MCC was shown in Figure 3(c); there are many irregular pores with diameter ranging from several nanometers to dozens of nanometers on the surface. The surface of MCC was smooth as shown in Figure 3(a), while the surface of MCC-g-PMMA looked like fish scale shown in Figure 3(b), which resulted from microphase separation. Comparing Figure 3(c) and (d), the grafted PMMA coating on the surface of MCC-g-PMMA could be obviously observed, the increased amount of irregular pores might be from the cracks of grafted PMMA after the soxhlet extraction.

TGA Analysis. The TGA technique was employed to characterize the thermal properties of the obtained graft copolymers, as shown in Figure 4. The weight loss was used to calculate the graft parameters, such as the graft ratio and polymer weight

fraction, as presented in Tables I and II. The thermal stability of graft copolymer can be compared at the onset temperature of decomposition and the percentage of weight loss for different stages of the decomposition. The onset temperature of decomposition is considered as an important parameter for thermal material properties since it strongly limits the application of materials.[51]

As shown in Figure 4, all of MCC-g-PMMA copolymers showed three decomposition stages. Compared to pure MCC, a new stage appears (stage three), which was attributed to the decomposition of grafted PMMA chains. The first decomposition stage of all the samples was attributed to the water evaporation. The MCC has 4.38 wt % of water. With increase in graft ratio, the water content was gradually decreased from 4.38 to 1.20 wt %. The second decomposition stages of copolymers were ascribed to the decomposition of MCC, the weight losses were decreased from 79.12% to 56.96% with increase in the graft ratio. The third decomposition stages of copolymers were assigned to the decomposition of grafted PMMA, the weight losses increased from 16.94% to 38.85% with increase in the graft ratio.

More information on thermal stability of MCC-g-PMMA copolymers could be obtained by investigation on the activation energy (E_a), as demonstrated by Broido method[52] and Coats and Redfern method.[53] Broido method is expressed as eq. (7).

$$\ln\left[\ln(1-\alpha)^{-1}\right] = -E_a/RT + const \tag{7}$$

where α represents the change in extent of reaction, E_a represents the activation energy, and T is the temperature. And Coats and Redfern method is expressed as eq. (8).

$$\ln\left[\frac{-\ln(1-\alpha)}{T^2}\right] = -\frac{E_a}{RT} + \ln\frac{AR}{qE_a}\left(1 - \frac{2RT}{E_a}\right) \tag{8}$$

where α represents the change in extent of reaction, E_a represents the activation energy, T is the temperature, A is the
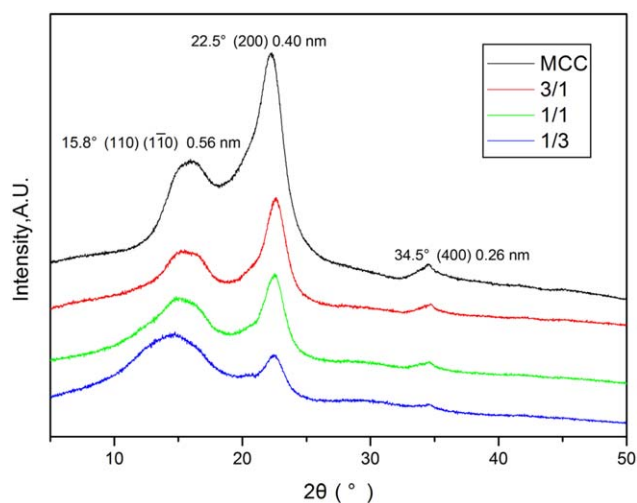

Figure 2. Wide-angle X-ray diffractions of MCC, MCC-g-PMMA 3/1, MCC-g-PMMA 1/1, and MCC-g-PMMA 1/3 after extraction. [Color figure can be viewed in the online issue, which is available at wileyonlinelibrary.com.]
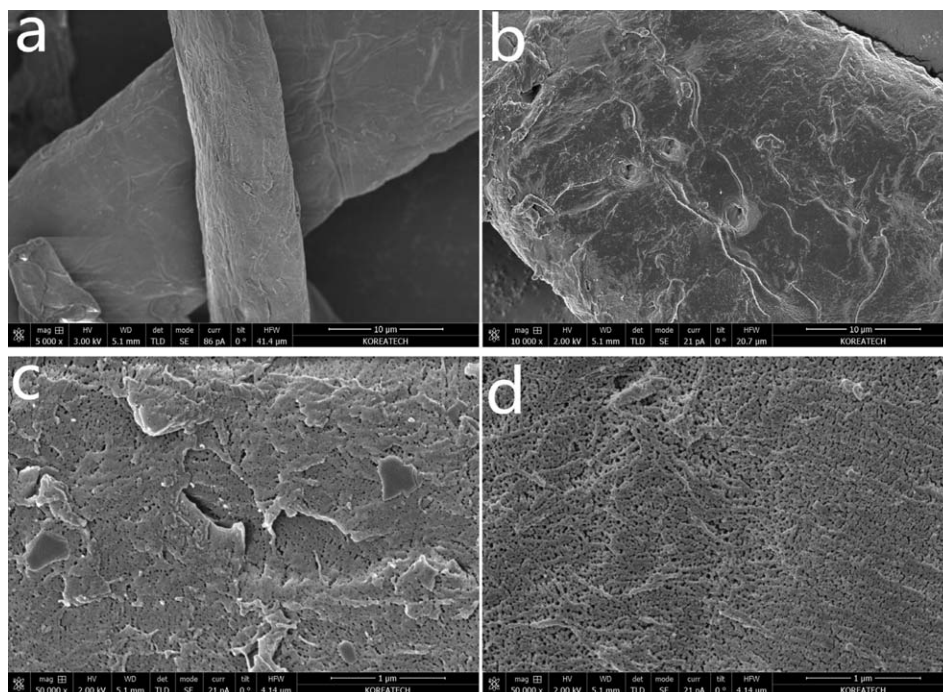
Figure 3. SEM photographs of (a) MCC, 10 μm, (b) MCC-g-PMMA 1/1 (after extraction), 10 μm, (c) MCC, 1 μm, (d) MCC-g-PMMA 1/1 (after extraction), 1 μm.
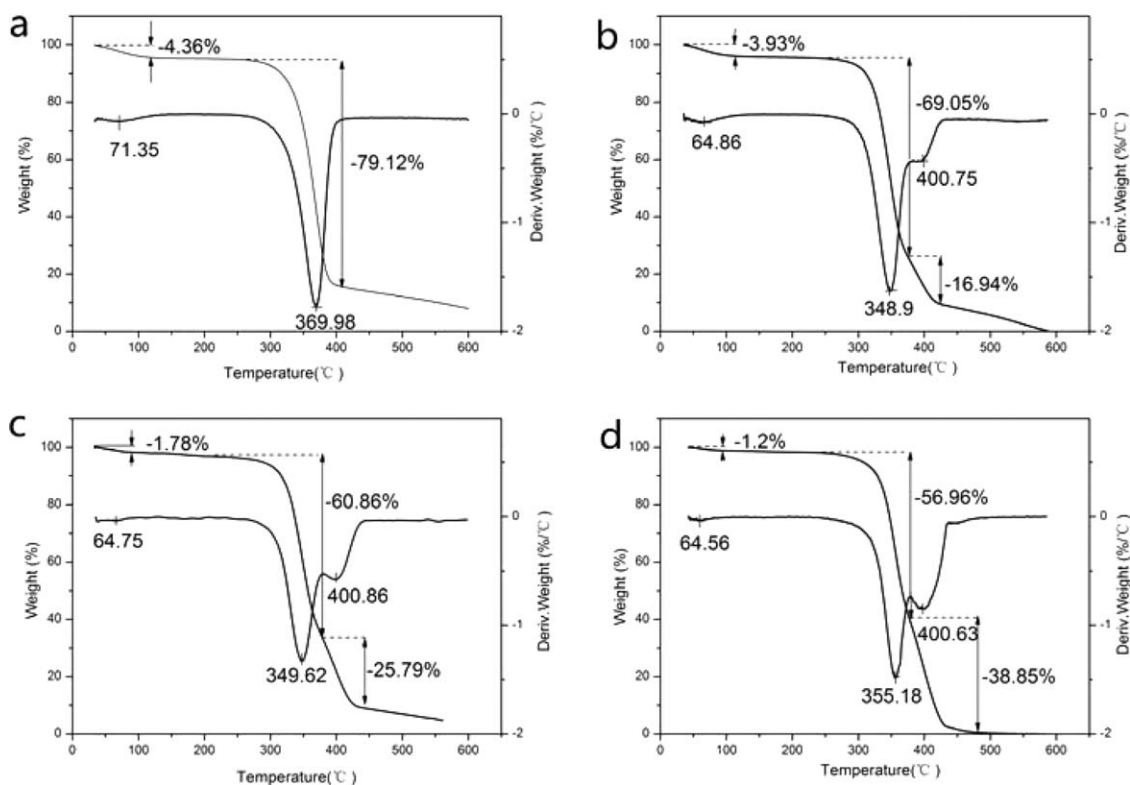

Figure 4. TGA and DTG thermograms of (a) MCC, (b) MCC-g-PMMA 3/1 (after extraction), (c) MCC-g-PMMA 1/1 (after extraction), and (d) MCC-g-PMMA 1/3 (after extraction).

Table III. Vulcanization Characteristics of MCC-g-PMMA/NR Composites

Samples	NR	MCC	MCC-g-PMMA 3/1	MCC-g-PMMA 1/1	MCC-g-PMMA 1/3
M_L (lb-in)	0.4	0.8	0.7	0.5	0.2
M_H (lb-in)	15.8	20.6	18.4	17.3	16.2
ΔH (lb-in)	15.4	19.8	17.7	16.8	16.0
ts_2 (min)	3.85	5.23	5.40	5.95	6.85
t_{90} (min)	8.17	9.78	10.12	10.40	11.08
CRI (min^{-1})	23.15	21.98	21.19	22.47	23.64

pre-exponential factor, R is the gas constant, and q is the heating rate.

With the Broido method, the E_a of MCC-g-PMMA (3/1, 1/1, 1/3) at the third decomposition stage were calculated as 50.72, 66.07, and 96.65 kJ/mol, respectively. With the Coats and Redfern method, the E_a of MCC-g-PMMA (3/1, 1/1, 1/3) at the third decomposition stage were calculated as 31.88, 47.22, and 77.81 kJ/mol, respectively. Thus, TGA analysis confirmed that the thermal stability of MCC-g-PMMA increased with increase in the graft ratio.

Characteristics of MCC-g-PMMA/NR Composites
Vulcanization Characteristics of MCC-g-PMMA/NR Composites.
The cure characteristics of MCC-g-PMMA/NR composites are summarized in Table III. The presence of MCC increased the torque values, including minimum torque (M_L), maximum torque (M_H), and the difference between minimum and maximum torque (ΔH). The increments in the torque values were due to the incorporation of rigid MCC, which strongly restricted the deformation and consequently increased the stiffness of NR composites. This is also evidenced by the change in the hardness of MCC/NR composites from 53.1 to 71.8 as shown in Table IV. In addition, the scorch time (t_{S2}) and optimum curing time (t_{90}) of MCC/NR were all prolonged due to the incorporation of MCC, which increased activation energy for vulcanization process. The vulcanization rate was indicated by curing rate index (CRI). It can be seen that the CRI values decreased from 23.15 to 21.98 owing to the incorporation of MCC, which affected the vulcanization process.

The torque values (M_L, M_H, and ΔH) of MCC-g-PMMA/NR composites decreased with increase in the graft ratio. The possible reason was that the glass transition temperature of PMMA is 105°C, so when the curing temperature was 140°C, the PMMA is elastic state. Additionally, the scorch time of MCC-g-PMMA/NR composites increased with the increase in the graft

ratio, owing to the larger size of copolymer with higher graft ratio. Furthermore the CRI values increased from 21.19 to 23.64 min^{-1} with the increase of graft ratio, which was higher than those of NR, due to the elastic state of PMMA at 140°C. From the results of vulcanization studies, it can be concluded that the grafted PMMA not only reduced the torque values, but also accelerated the vulcanization process.

Mechanical Properties of MCC-g-PMMA/NR Vulcanizates.
The mechanical properties of all samples were summarized in Table IV. It can be seen that the incorporation of MCC slightly increased the tensile strength, tear strength, and 300% modulus, while the elongation decreased. The copolymers showed stronger reinforcing effect on NR. The tensile strength of MCC-g-PMMA/NR increased with increase in the graft ratio, indicating that at higher graft ratio, the physical entanglement between grafted PMMA and NR was enhanced. However, the tear strength and 300% modulus of MCC-g-PMMA/NR both decreased with increase in the graft ratio. The reason was due to the decrease of stiff MCC in the copolymers.

The reinforcing mechanism of copolymers in NR matrix was as follows. The NR has self-reinforcing ability due to the strain-induced crystallization, so the mechanical properties were much better than styrene–butadiene rubber[54] and acrylonitrile butadiene rubber.[55] Therefore, the incorporation of reinforcing filler with a poor dispersion state is likely to weaken the self-reinforcing ability of NR, resulting in poor mechanical properties. As shown in Table IV, the tensile strength and tear strength slightly increased due to the extensive hydrogen bonds on the surface of MCC. However, the MCC-g-PMMA shows reinforced mechanical properties due to the physical entanglement of graft PMMA and NR macromolecules. Additionally, different graft ratio shows different reinforcing effect, lower graft ratio is better for improving the 300% modulus and tear strength, while higher graft ratio is better for improving the tensile strength

Table IV. Mechanical Properties of MCC-g-PMMA/NR Vulcanizates

Samples	NR	MCC	MCC-g-PMMA 3/1	MCC-g-PMMA 1/1	MCC-g-PMMA 1/3
Tensile Strength (MPa)	19.34	21.15	21.96	22.76	24.95
Elongation (%)	1320	1279	1287	1312	1424
300% Modulus (MPa)	1.591	1.715	1.932	1.862	1.766
Tear Strength (kN/m)	42.31	43.14	47.26	45.75	43.21
Hardness (Shore A)	53.1	71.8	71.2	70.2	68.7

and elongation. Therefore, it can be concluded that the MCC-*g*-PMMA was a better choice for rubber reinforcement compared to MCC.

CONCLUSION

MCC-*g*-PMMA was successfully synthesized in aqueous media using a redox initiated free radical polymerization, as confirmed by ATR, XRD, FE-SEM, and TGA analyses. The optimum reaction parameters were determined as MCC/MMA = 1/1; initiator concentration = 0.5 wt %; reaction temperature = 35°C; and reaction time = 3 h. MCC-*g*-PMMA showed enhanced thermal stability than neat MCC. MCC-*g*-PMMA and MCC were applied as filler to reinforce the NR matrix. Results showed that MCC-g-PMMA had better reinforcing ability than MCC, due to the formation of physical entanglements between grafted PMMA and NR. Furthermore, the incorporation of MCC-g-PMMA increased the torque values and CRI values. This research demonstrated the effect of reaction parameters on the grafting parameters and molecular weight of grafted PMMA, as well as the influence of surface modification of MCC on the vulcanization characteristics and mechanical properties of NR biocomposites, providing an alternative approach to develop high-performance rubber composites.

ACKNOWLEDGMENTS

REFERENCES

1. Schurz, J. *Progr. Polym. Sci.* **1999**, *24*(4), 481.

2. Li, M. C.; Wu, Q.; Song, K.; Qing, Y.; Wu, Y. *ACS Appl. Mater. Interfaces* **2015**, *7*(8), 5006.

3. Uesu, N. Y.; Pineda, E. A. G.; Hechenleitner, A. A. W. *Int. J. Pharma.* **2000**, *206*(1), 85.

4. Yu, X.; Atalla, R. H. *Powder Technol.* **1998**, *98*(2), 135.

5. Li, M. C.; Wu, Q.; Song, K.; Lee, S.; Qing, Y.; Wu, Y. *ACS Sustain. Chem. Eng.* **2015**, *3*(5), 821.

6. Battista, O. A. *Microcrystal Polym. Sci.* **1975**.

7. Abdelmouleh, M.; Boufi, S.; ben Salah, A.; Belgacem, M. N.; Gandini, A. *Langmuir* **2002**, *18*(8), 3203.

8. Dhakal, H. N.; Zhang, Z. Y.; Guthrie, R.; MacMullen, J.; Bennett, N. *Carbohydr. Polym.* **2013**, *96*(1), 1.

9. El-Saied, H.; Basta, A. H.; Hassanen, M. E.; Korte, H.; Helal, A. *J. Polym. Environ.* **2012**, *20*(3), 838.

10. Mishra, S.; Rani, G. U.; Sen, G. *Carbohydr. Polym.* **2012**, *87*(3), 2255.

11. Rani, P.; Sen, G.; Mishra, S.; Jha, U. *Carbohydr. Polym.* **2012**, *89*(1), 275.

12. Teramoto, Y.; Ama, S.; Higeshiro, T.; Nishio, Y. *Macromol. Chem. Phys.* **2004**, *205*(14), 1904.

13. Shen, D.; Yu, H.; Huang, Y. *J. Polym. Sci. Part A: Polym. Chem.* **2005**, *43*(18), 4099.

14. Roy, D.; Knapp, J. S.; Guthrie, J. T.; Perrier, S. *Biomacromolecules* **2007**, *9*(1), 91.

15. Carlmark, A.; Malmström, E. *J. Am. Chem. Soc.* **2002**, *124*(6), 900.

16. O'Connell, D. W.; Birkinshaw, C.; O'Dwyer, T. F. *J. Appl. Polym. Sci.* **2006**, *99*(6), 2888.

17. Littunen, K.; Hippi, U.; Johansson, L. S.; Österberg, M.; Tammelin, T.; Laine, J.; Seppälä, J. *Carbohydr. Polym.* **2011**, *84*(3), 1039.

18. Okieimen, F. E.; Ogbeifun, D. E. *Eur. Polym. J.* **1996**, *32*(3), 311.

19. Gao, J. P.; Tian, R. C.; Yu, J. G.; Duan, M. L. *J. Appl. Polym. Sci.* **1994**, *53*(8), 1091.

20. Gupta, K. C.; Khandekar, K. *J. Macromol. Sci., Part A* **2003**, *40*(2), 155.

21. Xiao, M.; Li, S.; Chanklin, W.; Zheng, A.; Xiao, H. *Carbohydr. Polym.* **2011**, *83*(2), 512.

22. Lanthong, P.; Nuisin, R.; Kiatkamjornwong, S. *Carbohydr. Polym.* **2006**, *66*(2), 229.

23. Lou, X.; Daussin, R.; Cuenot, S.; Duwez, A. S.; Pagnoulle, C.; Detrembleur, C.; Jérôme, R. *Chem. Mater.* **2004**, *16*(21), 4005.

24. Sakai, K.; Teng, T. C.; Katada, A.; Harada, T.; Yoshida, K.; Yamanaka, K.; Kunitake, M. *Chem. Mater.* **2003**, *15*(21), 4091.

25. Payne, A. R. *J. Appl. Polym. Sci.* **1962**, *6*(19), 57.

26. Shanmugharaj, A. M.; Bae, J. H.; Lee, K. Y.; Noh, W. H.; Lee, S. H.; Ryu, S. H. *Compos. Sci. Technol.* **2007**, *67*(9), 1813.

27. Kuang, T. R.; Mi, H. Y.; Fu, D. J.; Jing, X; Chen, B. Y.; Mou, W. J.; Peng, X. F. *Ind. Eng. Chem. Res.* **2015**, *54*(2), 758.

28. Li, M. C.; Zhang, Y.; Cho, U. R. *Mater. Des.* **2014**, *63*, 565.

29. Arrighi, V.; McEwen, I. J.; Qian, H.; Prieto, M. S. *Polymer* **2003**, *44*(20), 6259.

30. Ge, X.; Li, M. C.; Cho, U. R. *POLYMER-KOREA* **2014**, *38*(1), 62.

31. Zhang, Z.; Wu, Q.; Song, K.; Ren, S.; Lei, T.; Zhang, Q. *ACS Sustain. Chem. Eng.* **2015**, *3*(4), 574.

32. Zhang, Z.; Song, K.; Li, Y.; Wu, Q. *Int. J. Polym. Anal. Charact.* **2014**, *19*(4), 332.

33. Bras, J.; Hassan, M. L.; Bruzesse, C.; Hassan, E. A.; El-Wakil, N. A.; Dufresne, A. *Ind. Crops Prod.* **2010**, *32*(3), 627.

34. Bendahou, A.; Kaddami, H.; Dufresne, A. *Eur. Polym. J.* **2010**, *46*(4), 609.

35. Nunes, R. C. R.; Mano, E. B. *Polym. Compos.* **1995**, *16*(5), 421.

36. Amrtins, A. F.; Visconte, L. L. Y.; Nunes, R. C. R. *Kautschuk Und Gummi Kunststoffe* **2002**, *55*(12), 637.

37. Chuayjuljit, S.; Su-Uthai, S.; Tunwattanaseree, C.; Charuchinda, S. *J. Reinforced Plast. Compos.* **2008**.

38. Ismail, H.; Shuhelmy, S.; Edyham, M. R. *Eur. Polym. J.* **2002**, *38*(1), 39.

39. Zhang, W.; Zhang, X.; Liang, M.; Lu, C. *Compos. Sci. Technol.* **2008**, *68*(12), 2479.

40. Kato, H.; Nakatsubo, F.; Abe, K.; Yano, H. *RSC Adv.* **2015**, *5*(38), 29814.

41. Park, S. J.; Cho, M. S.; Lim, S. T.; Choi, H. J.; Jhon, M. S. *Macromol. Rapid Commun.* **2003**, *24*(18), 1070.

42. Zeng, C.; Lee, L. J. *Macromolecules* **2001**, *34*(12), 4098.

43. Li, M. C.; Lee, J. K.; Cho, U. R. *J. Appl. Polym. Sci.* **2012**, *125*(1), 405.

44. O'Brien, J. L.; Gornick, F. *J. Am. Chem. Soc.* **1955**, *77*(18), 4757.

45. Sen, G.; Kumar, R.; Ghosh, S.; Pal, S. *Carbohydr. Polym.* **2009**, *77*(4), 822.

46. Gupta, K. C.; Sahoo, S. *Biomacromolecules* **2001**, *2*(1), 239.

47. Gupta, K. C.; Sahoo, S.; Khandekar, K. *Biomacromolecules* **2002**, *3*(5), 1087.

48. Han, J.; Zhou, C.; Wu, Y.; Liu, F.; Wu, Q. *Biomacromolecules* **2013**, *14*(5), 1529.

49. Saito, T.; Isogai, A. *Biomacromolecules* **2004**, *5*(5), 1983.

50. Poletto, M.; Zattera, A. J.; Forte, M. M.; Santana, R. M. *Bioresource Technol.* **2012**, *109*, 148.

51. Li, H.; McDonald, A. G. *Ind. Crops Prod.* **2014**, *62*, 67.

52. Broido, A. *J. Polym. Sci. Part A-2: Polym. Phys.* **1969**, *7*(10), 1761.

53. Faria, E. A.; Prado, A. G. *React. Funct. Polym.* **2007**, *67*(7), 655.

54. Li, M. C.; Ge, X.; Cho, U. R. *Macromol. Res.* **2013**, *21*(5), 519.

55. Ge, X.; Li, M. C.; Cho, U. R. *Polym. Compos.* **2014**.